

Study of Bondura[®] Expanding PIN System – Combined Axial and Radial Locking System

Muhammad Maaz Akhtar¹ – Øyvind Karlsen^{1,2} – Hirpa G. Lemu^{1,*}

¹ University of Stavanger, Norway

² Bondura Technology AS, Norway

Bolted connections are widely used in parallel plates and flanged joints to axially lock using the preload generated by the tightening torque and to constrain radial movements of the flanges by the surface friction between mating surfaces. The surface friction depends on the micro-asperities of mating surfaces; under the influence of vibrations and other external radial loads, these asperities tend to deform over time, resulting in the failure of the connection. The Bondura expanding pin system presented in this article is an innovative axial and radial locking system, in which the failure of bolted connections due to radial movements is eliminated by relying on the mechanical strength of the pin system along with the surface friction. The present study describes an experimental design to verify the maximum possible preload on the axial-radial pin at different levels of applied torque. The article also provides a realistic comparison of the pin system with standard bolts in terms of handling axial and radial loads. With some alterations in the axial-radial pin system's design, the joint's capability to resist failure improved appreciably compared with the original design and standard bolts with higher preload. As a result, the estimated capability improvement of the joint against the connection failure due to the external radial load by the axial-radial pin is observed to be more than 200 % compared to standard bolts. Considering the pros and cons of both fasteners, i.e., axial-radial pin and standard bolts, a practical solution can be chosen in which both fasteners are used in a connection, and an optimized situation can be developed based on the working conditions.

Keywords: axial locking, expanding pin system, bolt preload, contact asperities, flanged connection, radial locking, shear resistance, shrink fit

Highlights

- The expanding pin technology that provides an innovative axial-radial locking system is described.
- The advantages of the innovative combined radial and axial locking system to eliminate the radial movement of bolted connections in flanges and pipes are studied.
- Experimental tests are conducted to verify the maximum possible preload that the axial-radial pin can generate at different applied torques.
- The shear capacity of a parallel plate joint using the axial-radial pin is compared with the capability of standard bolts of the same size.

0 INTRODUCTION

The flange connection is one of the most widely used pipe joints [1]; it involves bolts with nuts under pre-tension or preload. The preload in the bolts is generated by torquing the nuts that force the two flanges towards each other or by hydraulic tensioning of the shank and careful tightening of the nuts and realizing the hydraulic tensioning. This prevents axial movement of the flanges relative to each other, whereas the radial movements are prevented by the contact pressure between the mating flange surfaces under this preload [2] and [3].

Studies [4] show a direct relationship between the strength of the flanged joints and the level of the tightness. The drawback of this conventional practice comes from restricting the radial movements only on the shear resistance of the mating surfaces of flanges. The existence of minor radial movements can lead to total failure of the connection [5]. Further, in

pressurized big diameter pipe systems, leakage could occur because there always exist small vibrations in flange connections caused by the exposure to heavy loads and external vibrations caused by the flow of fluid [6]. These vibrations and radial movements reduce the surface friction between the bolt heads, nuts, and flanges by deforming the surfaces' micro-asperities and, eventually, it could cause a reduction in the preload, which could lead to failure of the connection [7]. In the presence of cyclic loading, bolted joints are one of the most exposed parts [8], and the fatigue performance of the joint is mostly governed by existing guidelines or standards, such as Eurocode recommendations [9], that are mostly conservative.

In flange-bolted joints, the thread friction and surface friction at the bearing surface of washers or nuts are influenced by the surface roughness, lubrication conditions, and the number of tightening and loosening events that influence the effectiveness of

*Corr. Author's Address: University of Stavanger, N-4036, Stavanger, Norway, Hirpa.g.lemu@uis.no

the joints to transfer the shear resistance. Furthermore, such connections require precise torquing to provide the necessary preload [10]. The tolerance that is kept between the diameter of the bolt and the bolt hole diameter of the flange for easy installation allows radial movements to occur. Theoretically, such a problem can be avoided by eliminating the tolerance by implementing an interference fit solution, such as press-fit or shrink-fit solutions [11] and [12].

Press-fitted solutions in bolted flange connections are challenging because obtaining a perfect match of all adjacent flange bores is quite difficult and often impossible, considering the combination of their sizes and positions. In addition to the installation difficulties, it would be challenging to retrieve the bolts without damaging the flange structure. In addition, applying press or shrink interference fit may be impossible to increase the contact pressure between the two main flanges due to the high friction contact pressure between the pins and flange bores. Tightening of the nut will possibly not overcome, or only partly overcome, the resistance due to contact pressure between the pin and the flange bore. In contrast, a shrink-fit solution could ease the installation compared to the press-fit, but it would suffer the same issues when it comes to tightening and retrieval [13].

Following this introduction section, this article is divided into five main sections. Section 1 describes the combined axial-radial locking system and the objectives of researching this invention. Then the

materials and methods used in the study are presented in Section 2, followed by the experimental setup in Section 3. The results of the experimental work are discussed in Section 4, and finally, the conclusions drawn from the investigation are presented in Section 5.

1 SYSTEM DESCRIPTION AND OBJECTIVES

To address the above-discussed problems with flanged joints, Bondura Technology AS has designed a technical solution for this rather complex problem with its “Expanding PIN System – Combined axial-radial locking system”, for which the company has received a Norwegian patent (number 344799). This pin system, which is currently in the design phase, has full potential to prevent connection failure due to the radial movements. This is because this pin system is designed to include the mechanical strength of the pin instead of just depending on the surface friction between mating surfaces of flanges.

For the application of the axial radial pin system, the connecting flanges or plates must be adopted accordingly by increasing the pin bore diameter partly through the flange, as shown in Fig. 1. The increased bore diameters are at the opposite flange faces compared to the mating flange faces. The axial radial pin system is symmetrical as illustrated by the three dimensional (3D) view in Fig. 1, which means the central pin is the centre of the pin system, and the

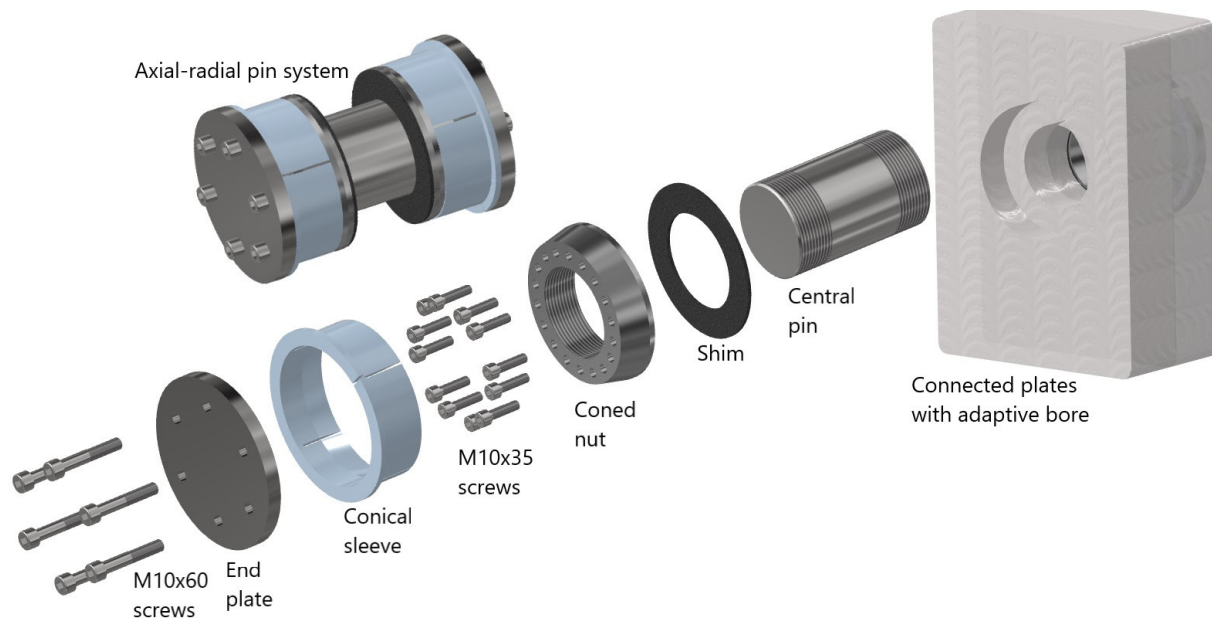


Fig. 1. Axial-radial pin system with exploded view and adaptive connecting plates

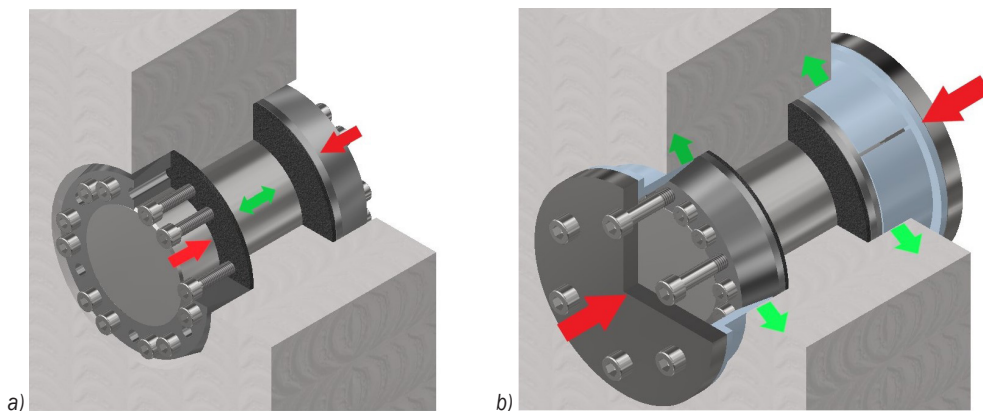


Fig. 2. Function of screws; a) M10×35, and b) M10×60

same six components are employed on both sides, as shown by the exploded view from one side.

In assembling, the central pin, which has threads on both ends, goes through the bolt holes of the flanges, and shims are inserted on both sides and placed at the bottom of the increased pin bore. The two coned nuts are then screwed by hand on each side of the central pin until both coned nuts touch shims.

The M10×35 screws are torqued through the coned nuts and create a pushing force on the flange surfaces, as shown by the red arrows in Fig. 2a. In reaction to the pushing force, the central pin, which is screwed by coned nuts on both sides, is tensioned to its final preload, indicated by green arrows in Fig. 2a.

After preloading the pin, the conical sleeves are installed on both sides of the central pin, which function as wedges to eliminate the radial tolerance between the pin system and the flange bore. End plates are used to transfer the force from the tightening of M10×60 screws into the coned nut to the conical sleeves, as illustrated in Fig. 2b.

Fig. 3 illustrates the difference between the design approaches to eliminate the failure of a flange connection by both fastener systems, standard and axial-radial pin systems. For the standard bolt and nut system, the restriction of both the axial and radial movements depends on the bolt's preload. If the preload is not sufficient or reduced over its functional period, the result would be loss of contact pressure, which could lead to the connection's failure.

For the axial-radial pin system, the restriction of the radial movements between the flanges does not entirely depend on the preload in the central pin. The expanded conical sleeve between the pin and flanges transfers the radial load to the central pin; for a failure to occur due to radial movements, the external radial

load must have sufficient magnitude to surpass the shear yield strength of the central pin.

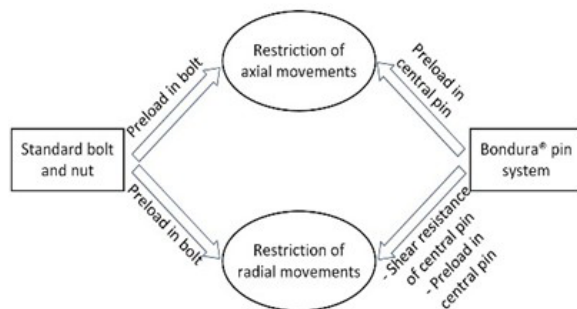


Fig. 3. Design approaches for axial-radial pin system and standard bolt in terms of restricting axial and radial movements

The work reported in this article is conducted as a collaboration project between Bondura Technology AS and the University of Stavanger as a part of a master's thesis [14]. As the axial-radial pin system with combined axial and radial locking system is in the testing and verification phase, theoretical, numerical, and experimental analyses are required to finalize and optimize the product. To optimize the product, two main objectives are identified: (1) investigate maximizing the preload in the axial-radial pin system as a function of numbers and sizes of tightening screws and factors that are limiting the maximum preload, and (2) to make a comparative study of axial-radial pin system with the standard conventional bolt system in terms of maximum preload and locking capability against radial and rotational movements.

Therefore, a study on both Ø50 mm and Ø80 mm axial-radial pin systems was conducted. In this regard, the maximum possible preloads for different torque levels were first estimated by using bolted connection theories [2] and [11]. An experimental setup was

designed for both pin systems to verify the calculated results. For the comparative study, two standard bolts, M50 and M80, were selected, and a comparison was made in terms of maximum possible preload and the ability to avoid failure emanating from radial movements. The experimental study is limited to the two sizes of axial-radial pin systems, i.e., Ø50 mm and Ø80 mm, which are provided by the company [15].

2 METHODS AND MATERIALS

Preload in bolted connection is possible by applying torque; to achieve the desired preload, it is important to understand the relationship between torquing level and resulting preload. The common method to define the relationship between maximum applied torque (T) and resulting preload (F_i) is given by the relation,

$$F_i = \frac{T}{Kd}, \quad (1)$$

where K is an experimental factor that is set equal to 0.18 for lubricated surfaces (on bearing surface and on threads) and d is thread diameter of the bolt/screw [2]. To verify the calculated preloads by an axial-radial pin system for different levels of applied torque according to the above equation, an experiment was designed in which different levels of torque are applied on both axial-radial pin systems. The purpose of the experiment was to observe the normal stress in the central pin. Therefore, instead of using a complete flange, a test jig was used, as shown in Fig. 4, which was bolted on the test bench.



Fig. 4. Experiment setup and manual application of torque on axial-radial pin system in the test jig

In this experiment, average normal stress along the central pin's longitudinal axis was measured using

two strain gauges of type KLY41 from HBM company [16], which were connected in parallel at an angle of approx. 180° on the pin. The reference temperature for this strain gauge is 23 °C, and the operating range for static analysis was from -70 °C to +200 °C. The strain gauge selected for this experiment has a grid length 3 mm and 200 Ω of grid resistance with a gauge factor of 2. The method employed in this experiment for the application of strain gauges is called the active dummy method [17]. It is a widely implemented method for compensating thermally induced strains. In this experiment, four strain gauges were used on a single pin, two of such strain gauges were applied on the central pin, and the other two were applied as dummy strain gauges on a member, which is made of the same material as of the central pin.

The used data acquisition system (DAQ) module is from HMB company and consists of a measurement electronics gadget known as Spider8 and software called Catman® professional [16]. For the application of controlled load, the torque in this experiment was applied by hand using a torque wrench from USAG company [18], as shown in Fig. 4. This torque wrench works on the turn-of-the-nut method and has an application range of 40 Nm to 200 Nm, which is sufficient for the present experiment because the maximum calculated torque that the M10 screw can sustain is approx. 147 Nm.

In terms of material, the end plate and conical sleeve are made of S355J2 with a minimum ultimate tensile strength of 450 MPa and a minimum yielding strength of 295 MPa, whereas the central pin, shim, and coned nut are made of 34CrNiMo6 material with a minimum ultimate tensile strength of 900 MPa and a minimum yielding strength of 700 MPa.

Furthermore, two sizes of ISO 4762 tightening screws were used in the pin system, (1) M10×35 screws with the property class of 12.9 with further hardening to property class 16.9 and (2) M10×60 screws with the property class of 12.9. Table 1 presents the tested material properties of the components.

3 EXPERIMENTAL SETUP

The test jig was bolted to the test bench with the M8 bolt and nut. Both M10×35 and M10×60 screws were lubricated prior to the testing. The central pin, which has two strain gauges bounded on it with the difference of approximately 180°, see Fig. 5, was inserted in the test jig, and then one of the shims was inserted on each side of the pin. Coned nuts were screwed on both sides of the pin, which were also lubricated for easy installation. By using the recommended

Table 1. Tested material properties of the components of both axial-radial pin systems

Component	Ø50 mm pin system		Ø80 mm pin system	
	Tensile strength [MPa]	Yield strength [MPa]	Tensile strength [MPa]	Yield strength [MPa]
Central pin	1083	978	1081	980
Shim	1858	1438	1858	1438
Conned nut	1494	1352	1494	1352
Conical sleeve	540	391	500	379
End plate	547	403	505	379
M10×35	1625	–	1625	–
M10×60	1293	–	1312	–

cross-pattern from ASME PCC-1-2010 [19], M10x35 screws were screwed on both sides consecutively with a torque wrench starting from 40 Nm, as it is the minimum limit of the torque wrench. Then, the torque is increased stepwise by 20 Nm until the first screw breaks. Real-time strain values were measured with the help of the DAQ.

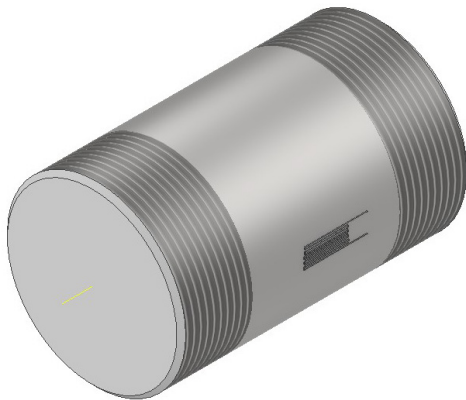


Fig. 5. Locations of the strain gauges on the central pin

Table 2. Measured strains in the central pin for different levels of applied torque

Torque levels [Nm]	Measured strain [µm/m]	
	Ø50 pin system	Ø80 pin system
0	0	0
40	368	222
60	609	312
80	873	416
100	1104	585
120	1366	676
140	1538	790

These measured strains are shown in Table 2 for both Ø50 mm and Ø80 mm pins for the given range of the applied torque levels. After setting the applied

torque to 160 Nm on the torque wrench, the screws broke for both pin systems.

4 DISCUSSION OF RESULTS

For the sake of comparison with experimental results, preload per screw was calculated at different torque levels, which is shown in Table 3. The Ø50 mm pin system contains 7 screws at each pin end, and there are 12 screws in the Ø80 mm pin system. Therefore, multiplication of the number of screws with the “preload per screw” results in the maximum possible preload of pin system, shown in Table 3 for both pin systems.

To validate the theoretical calculations by experimental results, the average normal stress in the central pin is calculated at different levels of torque by using the equation:

$$\sigma = \frac{F_t}{A_t}, \tag{2}$$

where A_t is the tensile stress area of the central pin and can be estimated by using [20],

$$A_t = \frac{\pi}{4} \times [d - 0.93815 \times p]^2, \tag{3}$$

where $p = 3$ mm is the pitch and d is the diameter of the central pin. Values of theoretical average normal stresses for both pin systems are shown in Table 3.

Measured strain values from Table 2 are utilized to calculate the average normal stresses by using Young’s modulus of $E = 210$ GPa for the central pin and the relationship between stress and strain. These relations are shown in Table 4 for different levels of the applied torque, along with percentage differences from the theoretical values. A positive difference means the measured value is higher than the theoretical value and vice versa for The negative difference. The average deviation of the experimental values from the theoretical values for Ø50 mm pin

Table 3. Theoretical values of preload per screw, max. preload, and normal stress for both axial-radial pin systems

Torque level [Nm]	Preload per screw [kN]	Ø50 mm pin		Ø80 mm pin	
		Max. Preload [kN]	Normal stress [MPa]	Max. Preload [kN]	Normal stress [MPa]
0	0	0	0	0	0
40	22.7	159.1	91.0	272.7	58.3
60	34.1	238.6	136.4	409.0	87.4
80	45.4	318.1	181.9	545.3	116.6
100	56.8	397.6	227.4	681.7	145.7
120	68.2	477.2	272.9	818.0	174.8
140	79.5	556.7	318.4	954.3	204.0
149.2	84.8	593.4	339.3	1017.3	217.4

Table 4. Calculated values of average normal stress from measured strains, and difference with theoretical stress

Torque level [N]	Ø50 mm pin		Ø80 mm pin	
	Normal stress from measured strain [MPa]	Difference from theoretical stress [%]	Normal stress from measured strain [MPa]	Difference with theoretical stress [%]
0	0	0	0	0
40	77.4	-14.9	46.5	-20.2
60	127.9	-6.3	65.4	-25.2
80	183.4	+0.8	87.4	-25.0
100	231.8	+1.9	122.8	-15.7
120	286.9	+5.1	142.0	-18.8
140	322.9	+1.4	165.8	-18.7

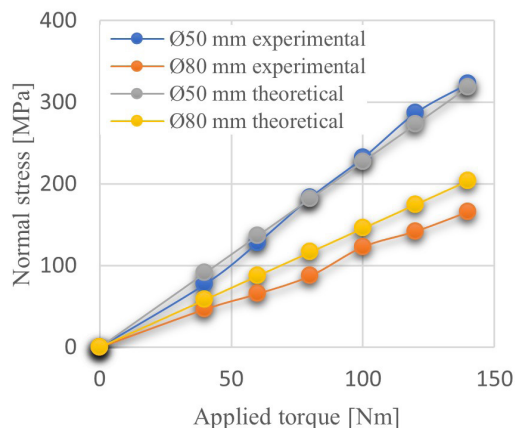
system is -2.0% with A standard deviation of 7.4 and for the Ø80 mm pin system is about -20.6% with a standard deviation of 3.8.

As illustrated in Fig. 6, there is a relatively good correlation between the theoretical values, given in Table 3, and the calculated values based on the strain measurements, Table 4, for both pin systems. However, the Ø80 mm pin reaches clearly a lower maximum pre-tension compared to that of the Ø50 mm pin. The reason is that when the pin diameter increases the number of tightening screws increases approximately linearly, but the cross-section area increases as a square of the pin diameter. The current design of both pin systems can be further optimized to yield higher preloads, which will be investigated later in this section.

For the Ø50 mm pin system, the values of measured strains are used only from strain gauge 1, due to an error incumbent while soldering the wires for strain gauge 2. Possible reasons for the deviation of the experimental values is the fact that, while applying torque, a fixture was used with torque wrench which might have absorbed some part of the torque.

As shown in Table 5, the calculated maximum preloads for the tested axial-radial pin systems are lower than the theoretical preloads for the standard bolts. Therefore, optimization is done regarding the

numbers and sizes of tightening screws of the axial-radial pin.

**Fig. 6.** Theoretical and experimental normal stresses vs applied torque for both pin systems**Table 5.** Maximum possible preload for both standard bolts and tested axial-radial pin systems

Fastener size [mm]	Standard bolt [kN]	Tested pin [kN]	Diff. [%]
50	1067.6	593.4	-44.4
80	2741.1	1017.3	-62.9

The preload in the axial-radial pin systems is contributed by the torque applied to the M10×35

screw; to increase the applied torque, the combination of screw size and number must be optimized. The experiment showed by increasing the torque on the M10 screws results in the breakage of the screw.

The number of M10×60 screws is limited to 4, and the clearance between the two bolt heads is fixed to 1.5 mm. Based on these conditions, a relationship is derived to estimate the maximum number (X) of M10×35 screws in axial-radial pin system as:

$$X = \frac{\pi d_B}{d_H + 1.5} - 4, \quad (4)$$

where d_B is the bolt circle diameter of coned nut and d_H is the bolt head diameter. This relation is used to estimate the number of different sizes of screws for both Ø50 mm and Ø80 mm axial-radial pin systems, as shown in Table 6. There is a geometrical restriction on the number of screws as the bolt head diameter should be less than the difference between the minimum outer diameter and inner diameter of the coned nut.

Considering the described geometrical restriction, the possible screw sizes for the Ø50 mm and Ø80 mm pin systems are M12 and M14, respectively. It was also found important to investigate the possibility of using smaller size screws than M10, when M8 screws were used. Using thread diameters of M8, M10, M12, and M14 according to ISO 4762 and minimum tensile strength of 1600 MPa and the relationship presented in Section 2 as Eq. (1), maximum torque and “preload per screw” was estimated; then the maximum preloads for both pin systems were calculated. All the calculated values are presented in Table 6.

Table 7 compares the preloads for improved axial-radial pin systems as a percentage difference between the standard bolt and the tested axial-radial pin system. The percentage difference is reduced significantly for both axial-radial pin systems as previously (Table 5).

As shown in Fig. 7a, the radial load is being applied on the connected flanges, leading to the relative radial movements, and this connection

Table 6. Theoretical max. possible preload for both axial-radial pin systems for different screw sizes and numbers

Size	Thread diameter [mm]	Max. torque [Nm]	Preload per screw [kN]	Ø50 mm pin system		Ø80 mm pin system	
				Max. number of screws [-]	Preload [kN]	Max. number of screws [-]	Preload [kN]
M8	7.78	74.0	52.8	11	581.0	18	950.8
M10	9.78	146.9	83.5	9	751.2	14	1168.6
M12	11.73	253.5	120.1	7	840.5	12	1440.9
M14	13.73	406.6	164.5	–	–	10	1645.1

Table 7. Comparison of preload for improved axial-radial pin system with standard bolts and tested pin system

Fastner size [mm]	Preload [kN]			Difference [%]	
	Standard bolt	Tested axial-radial pin	Improved axial-radial pin	Improved axial-radial pin vs std. bolts	Improved axial-radial pin vs tested pin
50	1067.6	593.4	840.5	-21.3	29.4
80	2741.1	1017.3	1645.1	-40.0	38.2

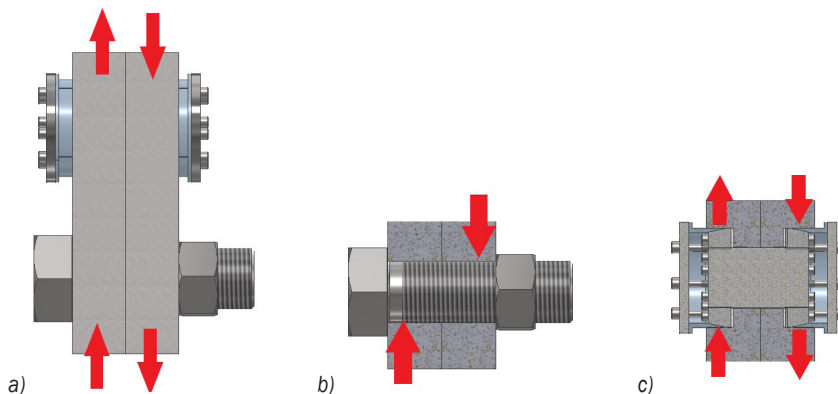


Fig. 7. Application of loads; a) Radial load on the connected flanges, b) radial load on a standard bolt, c) radial load on the conical sleeve of axial-radial pin system

contains both axial-radial pin system and standard bolt and nut. There is a surface resistance between mating surfaces of flanges, and it is acting in the opposite direction of the external radial load. This surface resistance is controlled by the permissible shear load or shear capacity and, according to Boris et al. [2], this shear capacity depends on the initial preload (F_i) and the coefficient of the friction (μ) between the mating surfaces of the flanges. This shear capacity is expressed as:

$$Q_p = \frac{F_i \mu}{k}, \tag{5}$$

where k is the factor of safety.

When the external radial load exceeds this shear capacity of a standard bolt, the external radial load starts to act freely on the bolt as shear load, as depicted in Fig. 7b. In contrast, the conical sleeves in the novel pin system are employed to make the connection as rigid as possible and to have a relative movement between connecting flanges. The external radial load applied on the conical sleeve, as shown in Fig. 7c, should be large enough to surpass the minimum shear strength of the central pin. This allows the inclusion of as another factor in the equation of shear capacity, which becomes:

$$Q_p = \frac{F_i \mu + \tau_y A_t}{k}, \tag{6}$$

where τ_y is the yield limit for shear strength of the central pin.

Eq. (5) is used to calculate the shear capacity of both standard bolts; the results are presented in Table 8, where the factor of safety is equal to 1. The values in this table do not account for the contribution of shear strength of bolt in the shear capacity of the connection.

Table 8. Theoretical shear capacity of both M50 and M80 standard bolts

Standard bolts	Maximum possible preload [kN]	Shear capacity [kN]
M50	1067.6	320.3
M80	2741.1	822.3

Table 9 presents the theoretical shear capacity of both axial-radial pins by using Eq. (6), along with the percentage increment of shear capacity in comparison to standard bolts. This increment illustrates the advantage of the axial-radial pin system over the standard bolt in terms of preventing the connection failure due to radial load. Here, the factor of safety is entirely dependent on the environmental condition of the flange joint, and it must be customized for each individual case, but for the sake of fair comparison, $k = 1$, $\mu = 0.3$, and $\tau_y = 450$ MPa.

Table 9. Theoretical shear capacity of both axial-radial pins and comparison of shear capacity increment

Pin size [mm]	Max. preload [kN]	Tensile area [mm ²]	Shear capacity [kN]	Shear capacity Inc. [%]
Ø50	840.5	1748.7	1043.0	225.7
Ø80	1645.1	4679.1	2599.1	216.1

Figs. 8 and 9 show comparative simulated situations between the axial radial pin system and standard bolt-nut connection, where two parallel plate connections are created by each fastener. In these simulations, an equal pressure load of 50 MPa as a radial load on each plate is applied in opposite directions, as shown in Figs. 8a and 9a, respectively. As expected, both fasteners have created the surface friction between plates, which are shown in Figs. 8b and 9b.

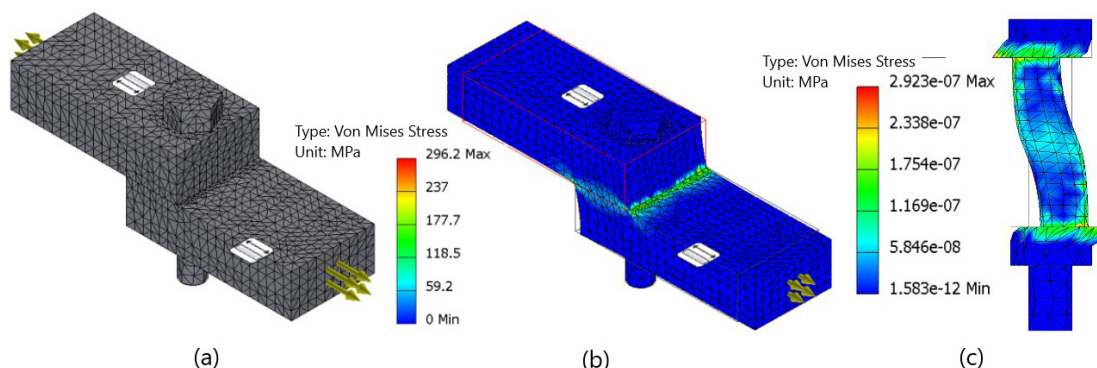


Fig. 8. a) Mesh view of the parallel plate connection by standard bolt and nut, b) surface friction between two plates, and c) isolated view of the bolt and nut

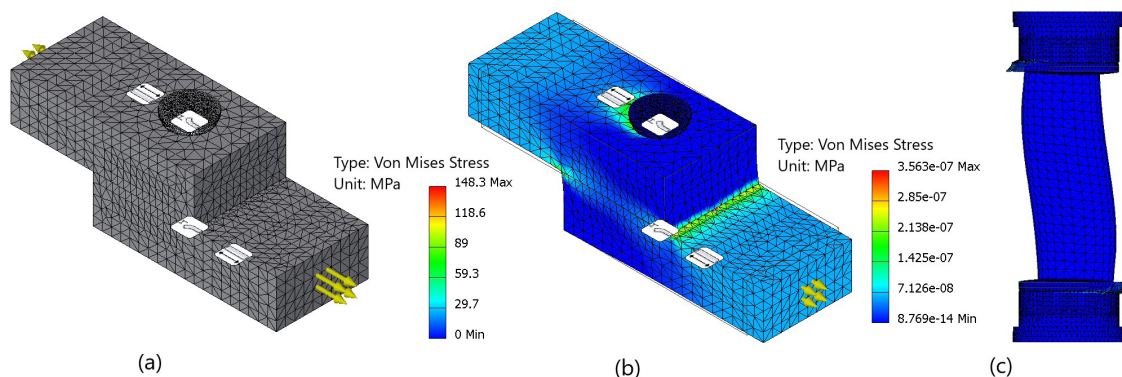


Fig. 9. a) Mesh view of the parallel plate connection by axial radial pin system, b) surface friction between two plates, and c) isolated view of the pin system

To understand the behaviour of both fasteners, they were isolated from the assembly and presented in Figs. 8c and 9c. In this case, the effect of the 50 MPa pressure is much disastrous for standard bolt-nut connection as there is major slipping in the high-stress areas (close to the bolt head and nut) as well as higher stress distribution in the centre of the shank, as compared to the axial-radial pin, where the relatively higher stress occurred in the conical sleeve, but the stress level in central pin is within elastic limit.

As shown in Table 10, the level of required torque to reach the maximum preload for each fastener is much higher for the standard bolt connection when compared to the axial-radial pin system connection. This is because torque is applied to several M12 and M14 screws in the axial-radial pin system, compared to high torque on a single M50 and M80 bolt for the standard bolts. Therefore, it is possible to apply torque by a simple torque wrench to the axial-radial pin system connection, whereas the standard bolt connection needs a high torque from a high-capacity torquing tool, typically hydraulic or electrical.

Table 10. Required torque for axial-radial pin systems and standard bolts to reach maximum possible preload

	Fastener	Required torque [Nm]
Axial-radial pin system	Ø50 mm /M12	253.5
	Ø80 mm /M14	406.6
Standard bolt	M50	9505.7
	M80	39106.8

Though the axial-radial pin system’s improved design can provide a higher preload than the tested design, it is still less than the preload per pin for the standard bolts. The axial-radial pins require more space per pin than the standard bolts, and fewer

pins will, therefore, fit on a defined flange system. To maximize the shear resistance for the complete flange system, it is, therefore, possible to apply a combination of standard bolts and axial-radial pins, for optimization purposes. The configuration can be decided by the design parameter responsible for radial movements.

5 CONCLUSION

With some deviation from the theoretical values, experiments confirm the maximum possible preload by both pin systems. In comparison with standard bolts of the same sizes, preload produced by an axial-radial pin system is lower than the standard bolt system, but with the presented changes in the initial design in this study, the difference in maximum preload is reduced significantly, 29 % in Ø50 mm pin system and 38 % in Ø80 mm pin system. The axial-radial pin has a locking mechanism based on the mechanical strength of the central pin. Theoretically, this locking system improves the capability of axial-radial pin connections by more than 200 % to avoid a failure due to radial loading as compared to the standard bolt connection. Along with that, the axial-radial pin requires significantly lower torque applied per screw as compared to standard bolts to obtain the maximum possible preload for a connection. Considering the advantages of the axial-radial pin in terms of capability to reduce or eliminate the failure due to radial loading and the ability of standard bolts to produce higher maximum possible preload, a practical solution is proposed, where a combination of both fasteners can be used to have a safe and secure flange connection. This expanding pin technology, particularly the axial-radial pin solution, is not well

known in the research community. With the results from this study, it is evident that the axial-radial pin solution is worth investigating further to obtain more knowledge about its potential, especially as a function of dimensions, material qualities and torque levels.

6 REFERENCES

- [1] Luan, Y., Guan, Z.-Q., Cheng, G.-D., Liu, S. (2012). A simplified nonlinear dynamic model for the analysis of pipe structures with bolted flange joints. *Journal of Sound and Vibration*, vol. 331, no. 2, p. 325-344, DOI:10.1016/j.jsv.2011.09.002.
- [2] Boris M.K., Barlam, D.M., Nystrom, F.E. (2008). *Machine Elements: Life and Design*. CRC Press, Taylor & Francis Group, Boca Raton.
- [3] Abid, M., Nash, D.H. (2003). Comparative study of the behaviour of conventional gasketed and compact non-gasketed flanged pipe joints under bolt up and operating conditions. *International Journal of Pressure Vessels and Pipes*, vol. 80, no. 12, p. 831-841, DOI:10.1016/j.ijpvp.2003.11.013.
- [4] Urse, G., Durbacá, I., Panait, I.C. (2018). Some research results on the tightness and strength of flange joints. *Journal of Engineering Sciences and Innovation*, vol. 3, no. 2, p. 107-130.
- [5] Takaki, T., Satou, K., Yamanaka, Y., Fukuoka, T. (2008). Effects of flange rotation on the sealing performance of pipe flange connections. *Proceedings of the ASME/JSME 2004 Pressure Vessels and Piping Conference*, DOI:10.1115/PVP2004-2630.
- [6] Ibrahim, R.A. (2010). Overview of mechanics of pipes conveying fluids-Part I: Fundamental studies. *Journal of Pressure Vessel and Technology*, vol. 132, no. 3, art. ID 034001, DOI:10.1115/1.4001271.
- [7] Bai, Y., Yang, M. (2016). The influence of superimposed ultrasonic vibration on surface asperities deformation. *Journal of Materials Processing Technology*, vol. 229, p. 367-374, DOI:10.1016/j.jmatprotec.2015.06.006.
- [8] Zhao, Y., Yang, C., Cai, L., Shi, W. Hong, Y. (2016). Stiffness and damping model of bolted joints with uneven surface contact pressure distribution. *Strojniški vestnik - Journal of Mechanical Engineering*, vol. 62, no. 11, p. 665-677, DOI:10.5545/sv-jme.2016.3410.
- [9] Eurocode 3 (2005). *Design of steel structures - Part 1-9: fatigue*. EN-2005.
- [10] Croccolo, D., De Agostinis, M., Vincenzi, N. (2011). Failure analysis of bolted joints: Effect of friction coefficients in torque-preloading relationship. *Engineering Failure Analysis*, vol. 18, no. 1, p. 364-373, DOI:10.1016/j.engfailanal.2010.09.015.
- [11] Chu, S.J., Jeong, T.K., Jung, E.H. (2016). Effect of radial interference on torque capacity of press- and shrink-fit gears. *International Journal of Automotive Technology*, vol. 17, p. 763-768, DOI:10.1007/s12239-016-0075-0.
- [12] Karlsen, Ø., Lemu, H.G. (2019). On modelling techniques for mechanical joints: Literature study. *International Workshop of Advanced Manufacturing and Automation*, vol. 634, p. 116-125, Springer, Singapore, DOI:10.1007/978-981-15-2341-0_15.
- [13] Chakherlou, T.N., Vogwell, J. (2004). A novel method of cold expansion which creates near-uniform compressive tangential residual stress around a fastener hole. *Fatigue & Fracture of Engineering Materials & Structures*, vol. 27, no. 5, p. 3423-351, DOI:10.1111/j.1460-2695.2004.00727.x.
- [14] Akhtar, M.M. (2020). *Expanding PIN System - Combined Radial and Axial Locking System*, MSc. Thesis, University of Stavanger, Stavanger.
- [15] Bondura AS, Bondura Technology. from <https://bondura.no/>, accessed on: 2021-06-30.
- [16] HBM. from: <https://www.hbm.com/en/>, accessed on: 2021-06-30.
- [17] Purwasih, N., Kasai, N., Okazaki, S., Kihira, H. (2018). Development of amplifier circuit by active-dummy method for atmospheric corrosion monitoring in steel based on strain measurement. *Metals*, vol. 8, no. 1, art. ID 5, DOI:10.3390/met8010005.
- [18] USAG company. Torque wrench with reversable ratchet. from: <https://www.usag.it/catalog/en/products/pdf/2309/Torquewrenches%20with%20reversibl%20ratchet.pdf>, accessed on 2021-06-30.
- [19] ASME (2010). *Guidelines for Pressure Boundary Bolted Flange Joint Assembly*. USA Patent ASME PCC-1-2010.
- [20] Norton, R.L. (2011). *Machine design: An integrated approach*, 4th Ed. Pearson Education Inc., New York.